International Journal of Electronics and Communications System
Volume 4, Issue 2, 71 - 85.
ISSN: 2798-2610
http://ejournal.radenintan.ac.id/index.php/IJECS/index
DOI: 10.24042/ijecs.v4i2.23618

Polarization and Phase Control of Electromagnetic Waves in Periodic and Quasiperiodic Photonic Crystals using Fullerene and Tellurium Nanolayers

Shalaw. S. Khalid*
Department of Physics, College of Science,
University of Halabja, IRAQ

Sana. L. Ahmed
Department of Physics, College of Science,
University of Halabja, IRAQ

Shene. A. Abdulrahman
Department of Physics, College of Science,
University of Halabja, IRAQ

Saman. O. Abdulla
Department of Physics, College of Science,
University of Halabja, IRAQ

Article Info

Article history:

Received: July 29, 2024
Revised: October 18, 2024
Accepted: November 29, 2024
Published: December 15, 2024

Keywords:

Elliptical polarization;
Fullerene;
Photonic crystal;
Transfer matrix method;
Photonic bandgap.

Abstract

This study presents the phase control and polarization of electromagnetic waves emitted in quasiperiodic crystals such as Fibonacci, T-M, DP, and RS and the periodic structure of a photonic crystal consisting of fullerene and tellurium nanoscales in near-infrared -visible wavelengths. By examining the arrangement of layers in quasi-periodic crystals, which, like periodic structures, possess band gaps that impede the transmission of electromagnetic waves, we can determine the specific region where the photonic band gap (PBG) is formed for both transverse electric (TE) and transverse magnetic (TM) polarization waves. Subsequently, after examining the transmitted light that passed through our structure, we have identified the band gap of different structures. Also, we have plotted the phase changes in the center and edges of the band gap. After taking into account the magnitude of the electric field and the phase difference, it becomes evident that when elliptically polarized light is transmitted, a tilt angle is seen corresponding to the angle of polarization. The paper used the renowned transfer matrix approach. According to our research, the suggested design enables the creation of very condensed phase controllers, such as phase retarders and polarizers.

To cite this article: S. S. Khalid, S. L. Ahmed, S. A. Abdulrahman, and S. O. Abdulla. "Polarization and Phase Control of Electromagnetic Waves in Periodic and Quasiperiodic Photonic Crystals using Fullerene and Tellurium Nanolayers, " *Int. J. Electron. Commun. Syst.*, vol. 4, no. 2, pp. 71-85, 2024

INTRODUCTION

The year 1987 saw the discovery of photonic crystals, sometimes known as PCs [1, 2]. Generally speaking, photonic band gaps (PBGs) are present in photonic crystals (PCs), which are periodic structures of electromagnetic media. The frequency ranges that these PBGs correspond to are those where light is unable to pass through the structure. The wavelength of the photons determines whether or not they are able to go through this structure. The most basic form of all the other structure types is the one-dimensional periodic structure. It consists of a series of layers with varying refractive indices, from low to high. The thicknesses of the layers are in accordance with the Bragg condition[3–5]. The whole PBG is shown by these wavelength bands, which are not permitted[6].

There has been a significant amount of attention in recent years towards the study of one-dimensional spatially periodic, quasi-periodic, and random photonic bandgap (PBG) structures, both in terms of their physics and practical applications[7–9]. The transition from the perfect periodic structure may be described using quasi-periodic systems, which can be considered to be

• **Corresponding author:**
Shalaw Saman Khalid, University of Halabja, IRAQ. ✉ shalaw.Khalid@uoh.edu.iq

acceptable models for this purpose[10]. One of the key tools in the fields of optoelectronics and contemporary optics is the photonic quasicrystal (PQC)[11]. Important examples of photonic quasicrystals are Thue Morse (T-M)[12,13], Fibonacci[14,15], Double Periodic (DP)[16,17], and Rudin Shapiro (RS)[18,19].

In 1985, Buckminster Fullerene (C60) was discovered, which not only brought about a breakthrough in the world of chemistry but also marked the beginning of the era of carbon nanotechnology[20]. First and foremost, Kroto conducted research on a particular organic molecule in space using a telescope that included precisely sixty carbon atoms that were located in close proximity to a number of red giant stars[21]. A Buckminster Fullerene, also known as C60, is a carbon-based structure consisting of hexagonal and pentagonal rings arranged in an enclosed spherical shape. The suffix "60" indicates the amount of carbon atoms present in the structure. Additionally, each carbon atom in the Buckminster Fullerene is sp2 hybridized. The structure includes around 20 hexagonal rings and 12 pentagonal rings[22]. In the realm of research and development, over the last decade, the chemical and physical properties of fullerenes have been a topic of interest and have received a lot of attention. This pattern is likely to persist for a lengthy period in the future since it is extremely likely that it will continue[23–25].

Fullerenes (C60) have garnered a lot of attention from the scientific community in recent times due to their new optical and electrical characteristics as well as their prospective uses. For example, fullerenes that have been doped with alkali metals can become superconductors, while thin films that have been doped can operate as conductors[23,26]. C60 fullerenes are quite simple to modify structurally, which is one of the reasons why the technical treatment is rather straightforward. Through the modification of the geometry and the degree of conjugation of the carbon superstructure, it is also possible to reproduce the electrical and optical characteristics of C60 fullerenes films. This may be done in order to get the desired results. It is possible to make use of this ability of C60 fullerenes in order to fabricate photonic crystal structures by making use of fullerenes filmsC60 thin films of exceptional quality have been successfully grown on a range of semiconductor and metal substrates, such as Te [27], Ge [28], GaAs [29], Ag [30] and so on. The near-infrared region and the wavelength range of 530 nm are the regions in which C60 thin films exhibit nearly little absorption [31]. It is also possible to disregard the dielectric constant in this region because it has very little impact on the frequency. In light of the fact that it is a metallic counterpart, in addition to having a dielectric constant that is practically frequency independent and a simpler fabrication procedure, it is advantageous in the design of the PC structure [32, 33].

The transfer matrix technique (TMM) is utilized in this study to calculate the transmittance and reflectance spectra, as well as to forecast the resonant frequencies and PBG properties. The transfer matrix method is known for its computational efficiency, accurate solutions in multilayer mediums, and adaptability across wave types and physical challenges. It thrives in multilayer materials and complicated refractive indices where other approaches may be less efficient or precise. The photonic structure is made comparing the arranged Thue Morse (TM), Fibonacci, double period (DP), Rudin Shperio (RS) quasi-periodic sequence with periodic structure in order to design an efficient Distributed Bragg reflector (DBR). We estimate an appropriate comparison in periodic and quasi-periodic structures with extremely high reflectivity. To produce an effective bandgap for both polarizations, we anticipate the degree of gap deformation as well as the wavelength and incidence angle parameters. We investigate the edge adjustment bar by altering the structure parameters. In addition, we introduce phase transitions at the boundaries. We show that the light that has linear polarization will change to elliptical polarization, and we show the tilt angle changes. The comparison of the optical and phase characteristics of four quasi-periodic stacking techniques and the conventional periodic structure, which may be used for devices that are needed, is an innovative aspect of the paper.

METHOD

Analysis of Periodic and Quasiperiodic Structures and Computational Techniques

All of the quasiperiodic structures taken into consideration in this study belong to the category that is often referred to as substitutional sequences. A number of subfields within the fields of computer science, mathematics, and cryptography have researched the sequences that are produced by replacements. Those applications in physics

that have been developed more recently have been described in the commencement. The characteristics of the sequences are determined by the characteristics of their Fourier spectrum, which may either be densely concentrated at particular points (seen in Fibonacci sequences) or display a continuous distribution with singularities (observed in T-M, DP, and RS sequences). Following in the footsteps of the articles that have previously used this methodology[34], we have also utilized it for the structure that is now being discussed. The nature of their Fourier spectrum determines the characteristics of the sequences.

Fibonacci

One of the most important factors that determines the presentation of a one-dimensional (1D) photonic crystal (PC) is its structure[35]. As non-Euclidean geometrical formations, Fibonacci fractal photonic crystal (FFPC) structures exhibit remarkable optical properties. A Fibonacci sequence transmission spectrum has forbidden frequency regions known as 'band gaps,' which are comparable to the band gaps shown in photonic crystals. Two isotropic dielectric materials, denoted by L and H, with thicknesses of $d_L$and d_H, respectively, and permittivity values of $\varepsilon_L$and ε_H. We assume that the layers have a permeability of $\mu_A\mu_H$ and that they are nonmagnetic. A recurrent relation determines the structure in each dielectric cell that follows the Fibonacci sequence, {□□=Sn-1-Sn-2}. The structure in every dielectric cell that follows the sequence determined by Fibonacci, {□□=Sn-1-Sn-2}, by a recurrent relation, where N is the Fibonacci unit cell's generation number, includes the following sequences.

S_2 =LH; S_3 =LHL; S_4 =LHHLH; S_5=LHLLHLHL; **etc**

The Fibonacci sequence of binary quasicrystal structure is one of the many quasiperiodic structures that has been the focus of significant research in recent decades. Since the discovery of the quasicrystal line phase in 1984, the electrical and optical characteristics of the Fibonacci multilayer structure have been extensively researched. This structure is a well-known example of a one-dimensional quasiperiodic structure. Fibonacci multilayer structures have been explored. A wave across a Fibonacci sequence structure has also been investigated in the last century; the Fibonacci sequence is characterized by resonant states that are located close to the band edge of a photonic structure[36].

Thue-Morse (T-M)

As a consequence of Thue-morse sequence research of aperiodic chains, which he began in 1906, the T-M series was first found. His findings have been rediscovered several times since then. Still, Morse's addition to the sequence in 1921, from the perspective of topological dynamics, is considered to be the most significant contribution to the sequence[37]. While there are other methods to define the T-M sequence, it is straightforward to demonstrate their equivalence. An alternative method to construct this series is by using the inflation rules L → LH and H → HL.

S_1→ L; S_2→ LH; S_3→ LHHL; S_4 → LHHLHLLH; etc. (1)

In this quasiperiodic system, the number of building pieces increases exponentially with n, specifically proportional to the value of 2n. Meanwhile, the ratio of the number of building blocks L to the number of building blocks H does not change and continues to be equal to one.

Double period (DP)

In the realm of aperiodic chains, the DP sequence is among the most recent examples[38]. Its inception may be traced back to the examination of system dynamics and the use of lasers in nonlinear optical fibers. The recursion relation has some resemblance to the T-M sequence scenario: the nth stage is determined by S0 → L and S1 → H. Additionally, it remains unchanged when subjected to the transformations L → LH and H → LL. The first cohorts include

S_0 = L; S_1 = LH; S_2 = LHLL; S_3 = LHLLLHLH; etc. (2)

The number of building pieces for the DP sequence grows proportionally to nth, following a pattern similar to the T-M sequence, namely doubling with each increment of n.

Rudin-Shapiro (RS)

It is an infinite automated sequence in mathematics that is referred to as the Rudin Shapiro sequence, which is also known as the Rudin Shapiro sequence. This series was named after Marcel, Walter Rudin, and Harold S. Shapiro, whose features were explored separately. In contrast to other sequences, such as the Fibonacci sequence, the Rudin-Shapiro sequence is peculiar in that it does not fulfill the requirements for a number of theorems that are applicable to a large number of quasiregular sequences. As a result, it displays distinct variances in the spectrum features. Additionally, it has a growth law for the number of component materials, which rises at a rate that is faster than that of other sequences, such as the Fibonacci sequence[8]. It is possible to create the Rudin-Shapiro arrays by using the two-letter inflation rule in the following manner:

LL →LLLH, LH →LLHL, HL→HHLH and HH→HHHL. The first generations are

S_0 = L; S_1 = LL; S_2 =LLLH; S_3 = LLLHLLHL; etc. (3)

Like the other described sequences, the number of building components for this sequence with n is double the value of n.

Periodic

The formation of periodic photonic structures is governed by fundamental deterministic rules, which also account for the formation of periodic structures[39]. In addition, the generating rule is carried out several times in order to produce:

S_1 =LH; S_2 =LHLH; S_3 =LHLHLHLH; etc. (4)

Transfer Matrix Method (TMM)

Our inspiration came from the use of the transmission matrix method (TMM) to compute the transmission spectrum and the notion of reflection[40]. The present investigation studies a one-dimensional periodic crystal composed of Fullerene (C60) and tellurium (Te) materials, which are subject to fundamental deterministic rules governing the formation of periodic photonic structures. The periodic photonic crystal consisting of alternating layers of C60 and Te may be constructed predictably by stacking the two building blocks, L and H. The stacking pattern is represented by S(Δz) = (LH)N, where L and H correspond to the layers of C60 and Te, respectively, and N indicates the number of lattice periods. Please refer to Figure 1 for a visual representation.

Furthermore, the generating rule is carried out several times in order to be generated. Figure 1 illustrates a one-dimensional quasicrystal and periodic structure arranged in a geometric pattern. This structure, known as a periodic multilayer construction, has been embedded in the air. The structure consists of many layers, with layers L and H expected to have thicknesses of dL and dH, respectively. Therefore, the L and H layers are considered to be positive-index isotropic materials.

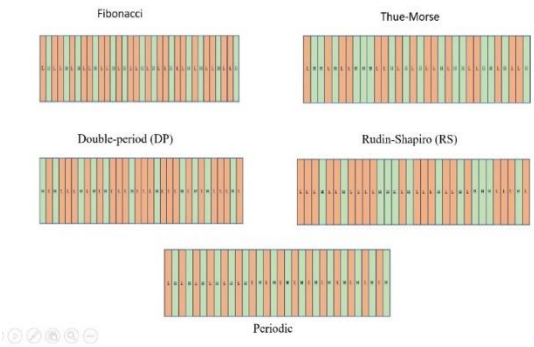

Figure 1 Schematic sketch of the one-dimensional structure, which is embedded in air. The thicknesses of L (C60) and H (Te) are supposed to be d_L and d_H, respectively.

The structural component in air consists of identical dielectric layers L and H, arranged in a periodic array along the z direction. In order to determine the transmission spectrum of a multilayer structure as a result of an electromagnetic wave impinging on the structure from the air at an angle of incidence θ, the transfer matrix approach is used. In the case of transverse magnetic (TM) and transverse electric (TE) waves, it is hypothesized that the electric field E and magnetic field H are orientated in the x direction and that the dielectric layers are located on the xy plane. Demonstrating the transfer matrix is possible.

$$M_j(\Delta z, \omega) = \begin{pmatrix} \cos(k_z^j \Delta z) & \frac{i}{\beta j}\sin(k_z^j \Delta z) \\ i\beta j \sin(k_z^j \Delta z) & \cos(k_z^j \Delta z) \end{pmatrix}, \quad (5)$$

Links the tangential components of the electromagnetic fields at the initial point of the jth layer to those at the final point of the layer. Here, $k_z^j = (\omega/c)\sqrt{\epsilon_j}\ \sqrt{\mu_j}\sqrt{1 - sin^2\theta/\epsilon_j\mu_j}$ is the component of the wave vector along the z-axis in the jth layer, $\beta_j = (k_z^j/\omega\epsilon_0\epsilon_j)$ for transverse magnetic field (TM) wave, where ϵ_0 is the permittivity of the vacuum, and $\beta_j = (k_z^j/\omega\mu_0\mu_j)$ for transverse electric field (TE) wave where μ_0 is the permeability of vacuum, c is the speed of light in vacuum. The 2 x 2 matrix is called the matrix of the film, represented generally by:

$$M = \begin{pmatrix} M_{11} & M_{12} \\ M_{21} & M_{22} \end{pmatrix}, \quad (6)$$

The reflection and transmission coefficients may be expressed in terms of the transfer matrix elements to get a solution.

$$r = \frac{\gamma_0 M_{11} + \gamma_0\gamma_s M_{12} - M_{21} - \gamma_s M_{22}}{\gamma_0 M_{11} + \gamma_0\gamma_s M_{12} - M_{21} + \gamma_s M_{22}} \quad (7)$$

$$t = \frac{2\gamma_0}{\gamma_0 M_{11} + \gamma_0\gamma_s M_{12} - M_{21} + \gamma_s M_{22}} \quad (8)$$

where we have writing

$$\gamma_0 = n_0\sqrt{\epsilon_0\mu_0}\cos\theta_0 \quad (9)$$

$$\gamma_s = n_s\sqrt{\epsilon_0\mu_0}\cos\theta_s \quad (10)$$

and the total reflectance and transmittance

$$T = |t|^2 \quad (11)$$

$$R = |r|^2 \quad (12)$$

The treatment of TE waves is similar to that of TM waves [41].

An investigation was conducted on the polarization characteristics of a one-dimensional quasicrystal dielectric multilayer structure (see Fig. 2). The tilt angle is the angle of rotation, measured counterclockwise, from the x-axis to the semi-major axis of the ellipse. Due to the symmetrical features of the ellipse, the tilt angle only has to be specified within the range of $-\pi/2$ to $\pi/2$. The tilt angle may be determined by establishing a rotated coordinate system in which the semi-major and semi-minor axes are aligned with the rotated coordinate axes.

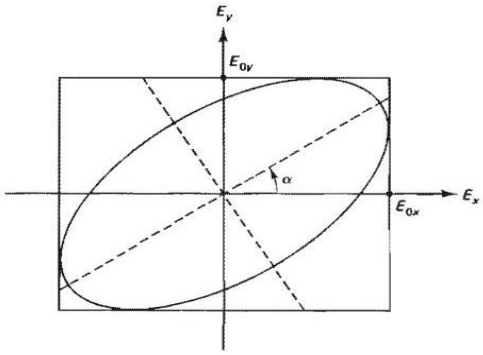

Figure 2*. The polarization ellipse shows fields Ex and Ey and azimuthal angle α. The tip of the electric field E traces this elliptical path in the transverse plane as the field propagates down the z-axis.*

We assume that we use linearly polarized light on the structure, taking note of the variations in phases and amplitudes of the field that affect the polarization reflected in the ellipse. What is the angle between the x-axis and the form of the ellipse? Thus, the solution of tilt angle takes the form:

$$\tan 2 = \frac{2E_{0x}\,E_{0y}\cos\varepsilon}{E_{0x}{}^2 - E_{0y}{}^2} \quad (13)$$

Where $\Delta\varphi = \varphi_{TE} - \varphi_{TM}$ Notice that you can rewrite this equation strictly in terms of the amplitude ratio and the phase difference, Let the of E along the x-and y-axes be E_x and E_y, respectively[42].

RESULTS AND DISCUSSION

Over the past several decades, research on photonic crystal (PhC) devices has always been a popular field of study[43–45]. As a result of the unique photonic band gap (PBG), electromagnetic waves that are in a certain frequency range, as well as controlling the phase of waves in different areas of the electromagnetic wave spectrum, were able to obtain different polarizers[46]. The numerical outcomes of different physical parameters for an electromagnetic wave moving through Fibonacci, Thue-Morse, Rudin Shapiro, Double Period, and periodic structures. The 1D photonic quasicrystal multilayer stacks are presumed to be situated inside an air medium. The components that make up the photonic quasicrystal are characterized as being linear, homogenous, and transparent. This study is being conducted with the intention of determining the ways in which the

accumulation of layers on the periodic structure and the quasi-periodic structure influences the establishment of the band gap and phase changes. The ultimate goal of this research is to discover a method by which the phase may be controlled.

The bandgaps that are seen in the properties of the multilayer material are subjected to extensive analysis for a variety of crystal parameters at a variety of generation numbers of quasi-periodic sequences and periodic structures. These materials are set to be the Fullerene C_{60} and the Tellurium (Te), with refractive indices $n_{C_{60}}$ = 2.1 and n_{Te} = 4.8, respectively. The thickness of the bilayers (d_L = 60 nm and d_H = 40 nm) and the arrangement of the number of different layers in C_{60} and Te. We have assumed that the number of layers for the structure that we are considering is 32 layers; however, only the Fibonacci 34 layers are taken into consideration. This second figure shows the transmission bands band structure in perpendicular directions θ=0° for TE waves, as well as the numerical analysis of the proposed computer settings. The transmission matrix method is used to model the transmission through this thin multilayer film. It can be seen from Fig. 3 that the center wavelength of the band structure for periodic 650nm, Fibonacci 825nm, Thue-Morse 980nm, Double Period 580nm and Rudin Shapiro 810nm. In this article, the letters (a) are related to the Fibonacci structure, (b) Thue-Morse's, (c) Double Period, (d) Rudin Shapiro, and (e) Periodic sequence, respectively.

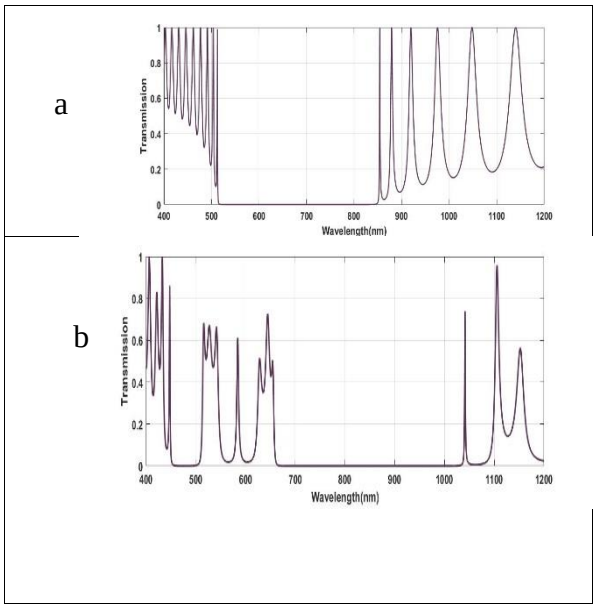

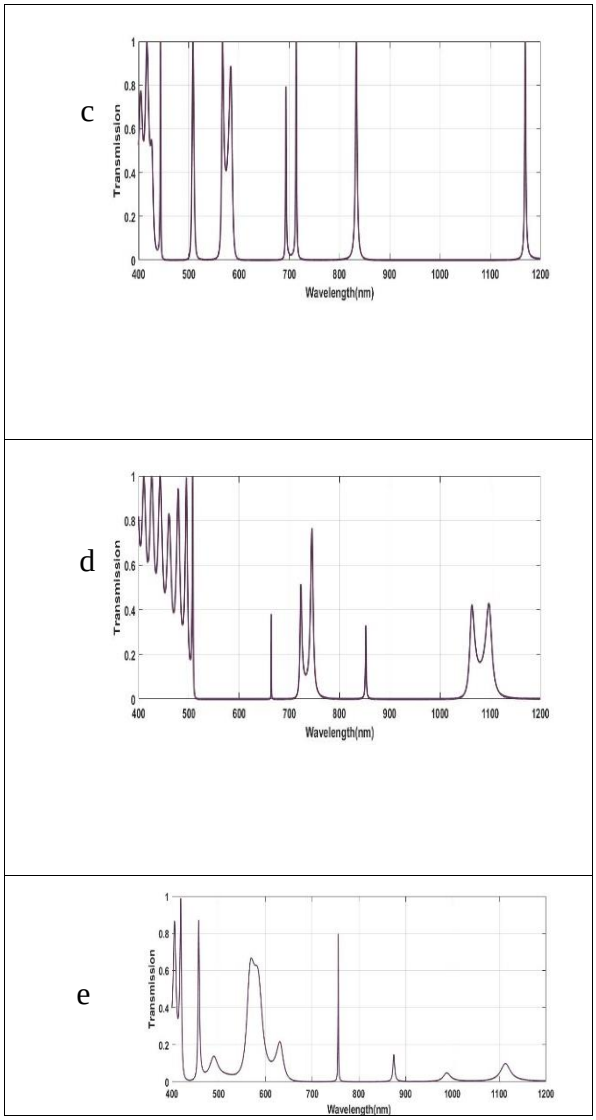

Figure 3. Band structure of the TE mode in one-dimensional fullerene-Tellurium nanocomposite structure at different central wavelengths: (a) periodic (b)Fibonacci (c) Thue-mors (d) Double period (e)Rudin shape.

In Figure 3, we have selected the largest band gap for both TE and Figure 4 TM polarizations. The light transmission spectra versus the resonant frequency $\Omega_0/2\pi$, for different one-dimensional quasiperiodic sequences along with periodic structure are presented in Fig. 3 for a different incident angle ($\theta^0 = 0^\circ$, $\theta^0 = 30^\circ$, $\theta^0 = 60^\circ$). Here, the quasiperiodic sequences with generation number considered are as follows: 8th generation of Fibonacci sequence, 5th generation of Thue-morse, Double period and Rudin Shapiro sequence, 5th generation of Periodic sequence, respectively. The generation numbers are chosen to get the multilayer consisting of nearly the same number of slabs, i.e., 99 slabs, The point at

which the band interval can be seen for the manufacturing number that corresponds to it. A band was seen in the near-infrared spectrum, which extends from 655 nm to 1040 nm, in relation to the Fibonacci sequence. Similarly, for the Thue-morse sequence 833nm to 1169nm, Double period 507nm 664nm, Rudin Shapiro 755nm to 874nm and Periodic structure 512nm to 855nm, respectively.

The fourth figure displays the transmittance spectra of a 1D multilayer sequence consisting of fullerene-germanium double periods. The spectra are shown for TM polarizations (Fibonacci, T-M, DP, RS, Periodic) in the visible to near-infrared wavelength range. The spectra are plotted for different angles of incidence: 0^0 (solid line), 30^0 (dashed line), and 60^0 (dotted line).

According to these figures, the transmission spectra of C60-Te display a band gap for both TE and TM waves throughout the visible wavelength range of around 490nm to 720nm. This band gap is present for both varieties of waves. Furthermore, the upper and lower borders of the gap move towards longer wavelengths as the angle of incidence rises for both TE and TM polarizations. This occurs regardless of whether the polarization is TE or TM.

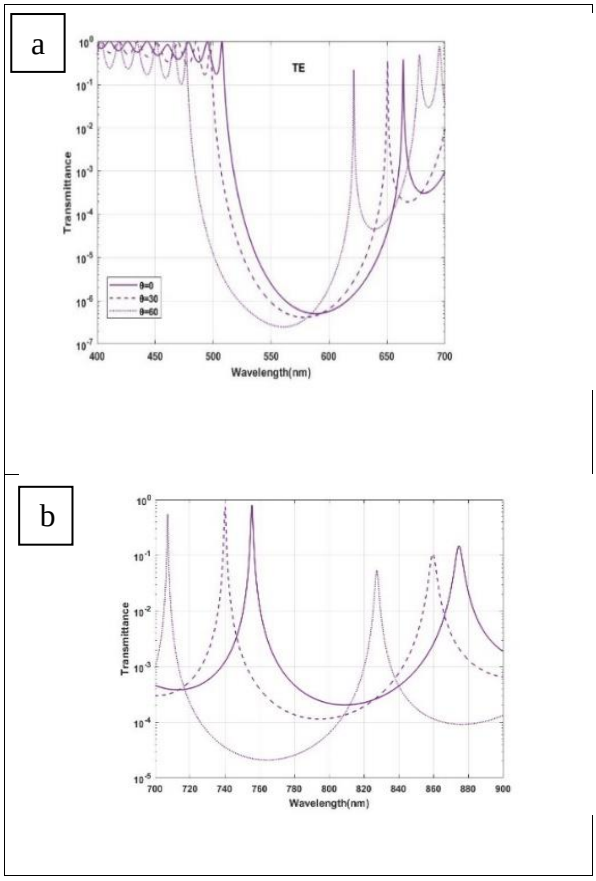

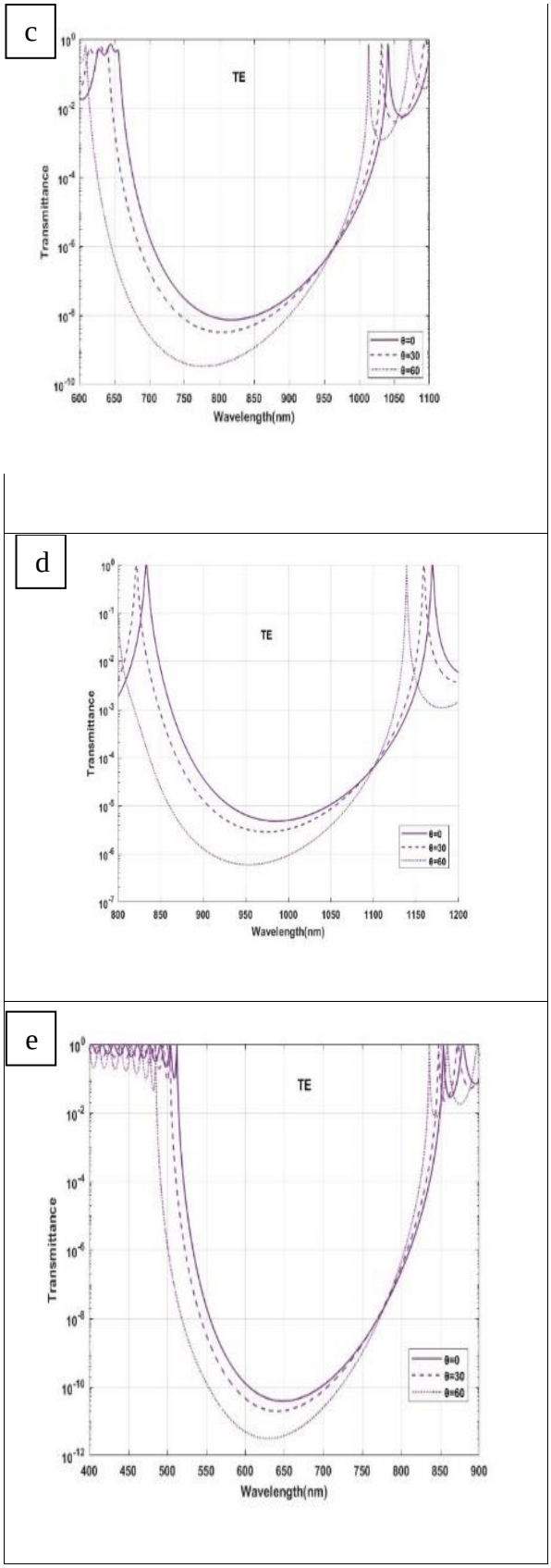

Figure 2. Transmission spectra of (a) Fibonacci, (b) T-M, (c) DP, (d) RS, (e) Periodic structure fullerene and Te for TE modes at a different angle of the incident as 0^0 (solid line), 30^0(dashed line), and 60^0(dotted line).

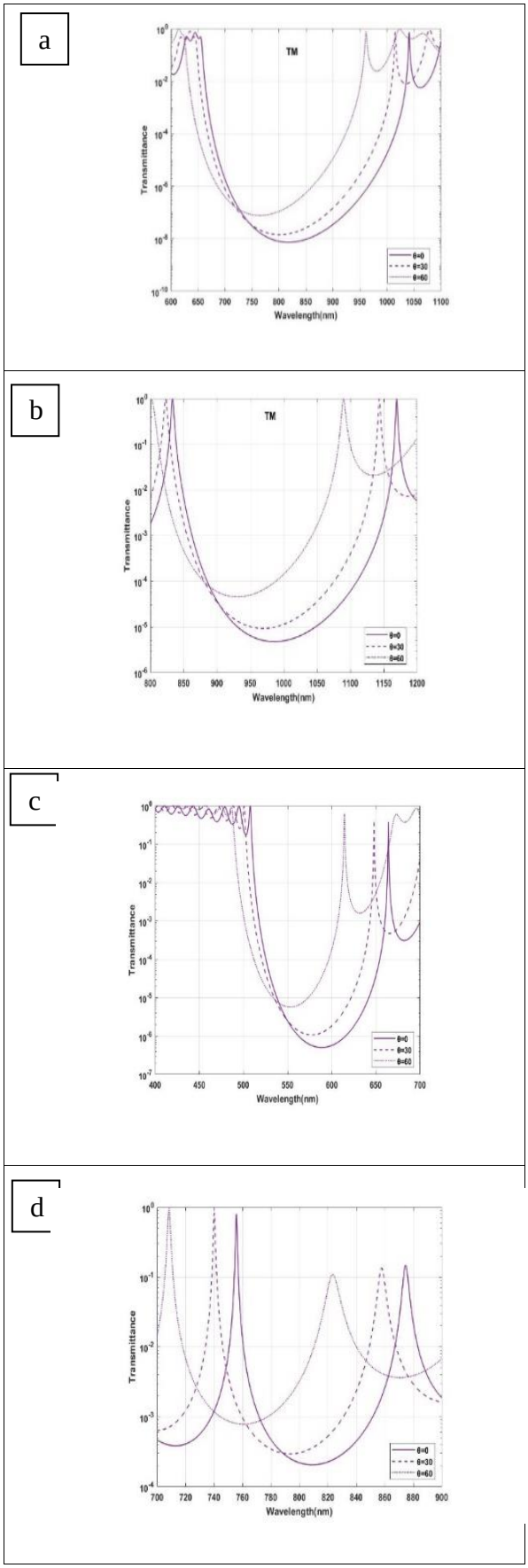

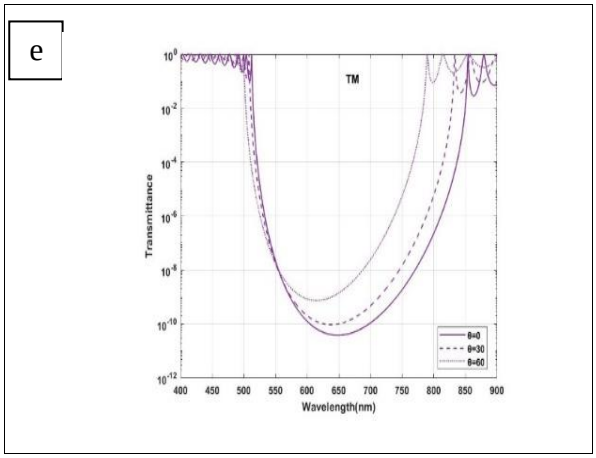

Figure 3. Transmission spectra of a) Fibonacci, (b) T-M, (c) DP, (d) RS, (e) Periodic structure fullerene and Te for TM modes at a different angle of the incident as 0^0 (solid line), 30^0(dashed line), and 60^0(dotted line).

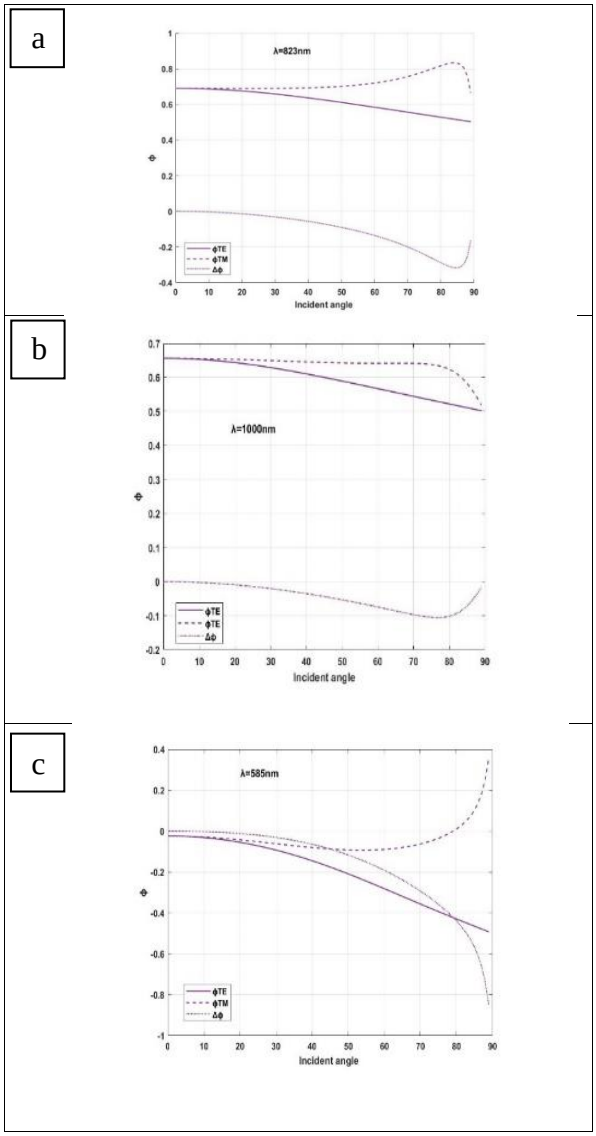

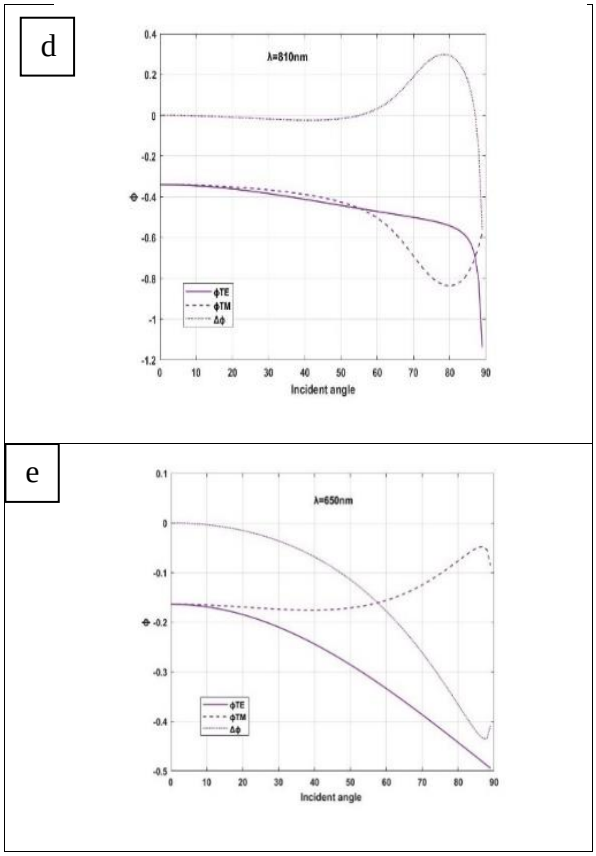

Figure 4 determined the phase difference between the TE and TM modes' phase shifts as a function of the incidence angle in the fullerene-Te multilayer structure's stop band for both the quasiperiodic and periodic structures

Now, what kind of an effect does this have on the phase difference that exists between the bands at the higher, lower, and center wavelengths? Am I able to change it? As a means of responding to this query, we investigate the connection between the phase difference of two transmitted waves with TE and TM polarization at the gap's borders and the phase difference of the reflected waves in the gap's center. This gives us the opportunity to answer the issue. Our investigation also encompasses the examination of the variation in the phase difference ($\Delta\varphi = \varphi TE - \varphi TM$) as the wavelength changes. As the incidence angle fluctuates within the stop band for the center band wavelength, Figure 4 depicts the phase difference that occurs between the phase shift of TE polarization and TM polarization because of the variation in phase. In addition, the fullerene-Te arrangement has a center band wavelength Fibonacci (λ=823 nm), T-M(λ =1000 nm), DP(λ =585 nm), RS(λ =810 nm) and Periodic (λ =610 nm).

Our calculations indicate that variations in wavelength and incidence angle result in slower changes within the stop band. Furthermore, when the incidence angles are near zero, the disparity in phase shifts between TE and TM waves is very negligible and remains unaffected by the incident angle. However, as the incident angle grows, this disparity starts to vary.

The study aimed to ascertain the tilt angle of a periodic structure and one-dimensional Fullerene and Tellurium quasicrystal dielectric multilayer, as seen in Figures 6 and 7. We hypothesize that we use the wavelength of light at the lower and higher ends of the spectrum to analyze the band structure. This takes into account the variations in phases and amplitudes of the field, which affect the polarization of light as it is reflected and transmitted through an elliptical medium. What is the tilt angle between the x-axis and the formed ellipse? We have identified the two edges of the band gap and have chosen the first, last, and center wavelength bands with the widest range of passage.

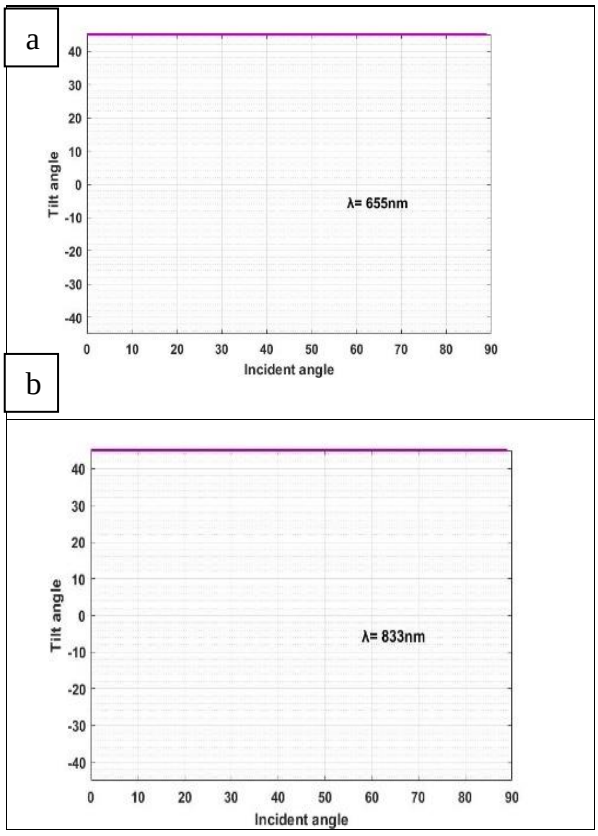

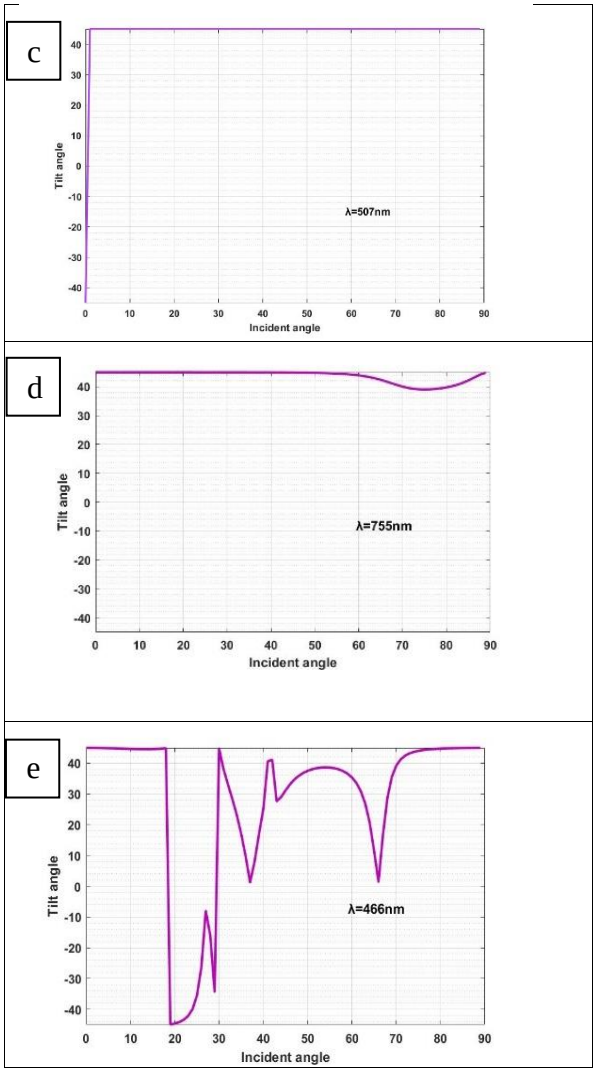

Figure 5. The lower edge's tilt angle of transmission in relation to the entering light's wavelength Fibonacci (λ=655nm), Thue Morse(λ=833nm), Double Period (λ=507nm), Rudin Shapiro (λ=755nm), Periodic (λ=466nm).

The lower band edge wavelengths are as follows: Fibonacci (λ=655 nm), T-M (λ=833 nm), DP (λ=507 nm), RS (λ=755 nm), and Periodic (λ=466 nm). The higher band edge wavelengths are as follows: Fibonacci (λ=1041 nm), T-M (λ=1169 nm), DP (λ=664 nm), RS (λ=874 nm), and Periodic (λ=855 nm). Equation (2) may be used to get the tilt angle α based on the angle of incidence θ. Note that for all three low and higher band structures, light transmission has the highest value in those two points of our spectrum. Consequently, the following inequality restricts the tilt angle of the elliptical polarization: −45° <□< 45. In the cases of lower edge band structure Fibonacci, T. Morse, and Double Period, it is evident that the tilt angle, which is 45 degrees, does not vary when the incidence angle increases.

On the other hand, in the case of Rodin Shapiro, the entrance angle will shift by 60 degrees. Throughout the period structure that occurs after the incidence angle of 18 degrees, the tilt angle goes through a series of quick variations that vary from 45^0 degrees to -45^0 degrees. The dependency of tilt angle on the angle of incidence is seen in Figure 7, which may be found attached here. With the rise in the descent angle, we have shown that the tilt angle has not altered solely in Rudin Shapiro; rather, it has stayed at 45 degrees throughout the process. Other structures, such as the Fibonacci and T-Morse structures, as well as the double period and periodic structures, have tilt angles that are very sensitive to the angle at which they are impacted. The center edge's tilt angle of reflection in relation to the entering light's wavelength can be seen in Figure 8.

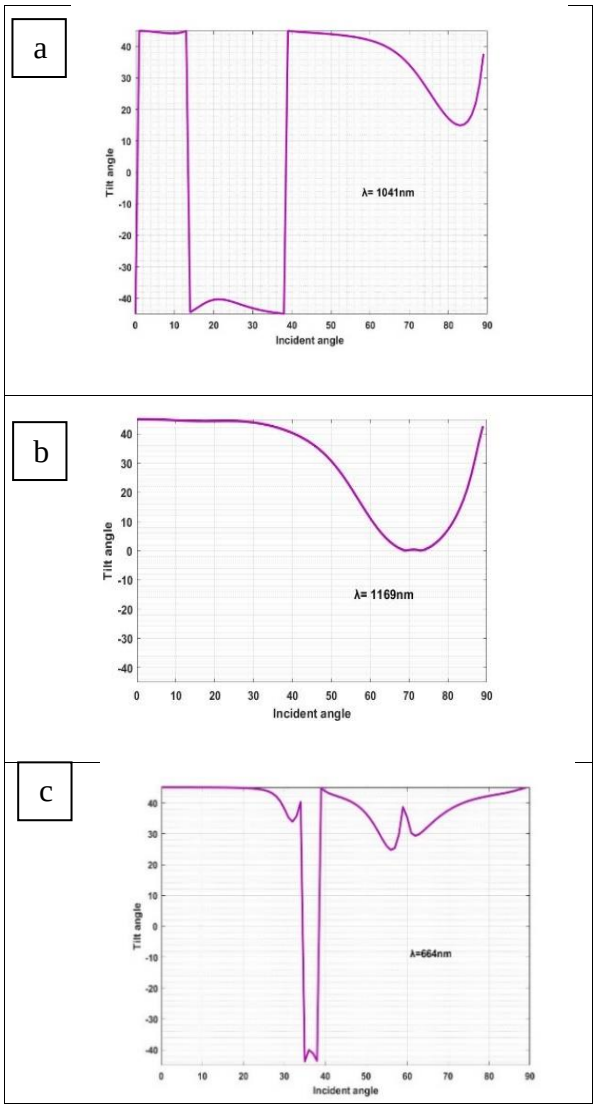

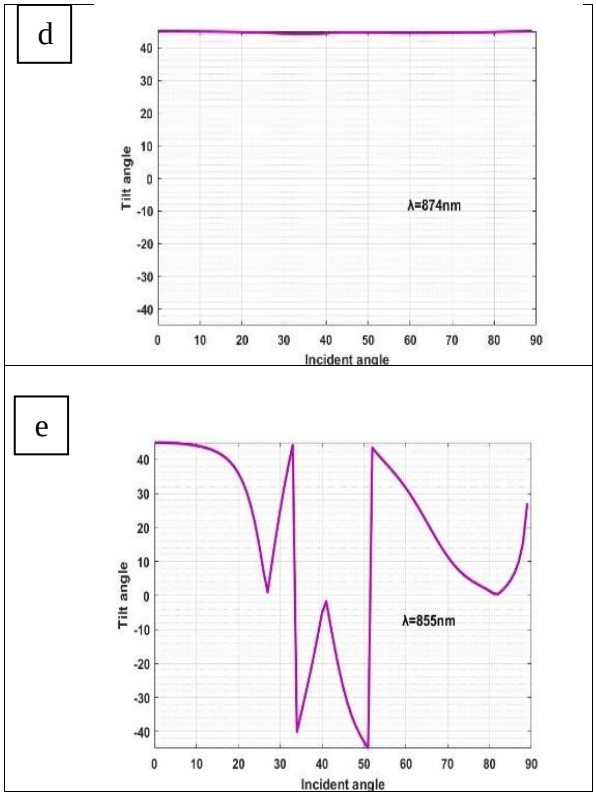

Figure 6. The higher edge's tilt angle of transmission in relation to the entering light's wavelength Fibonacci (λ=1041nm), Thue-Morse (λ=1169nm), Double Period (λ = 664 nm), Rudin Shapiro (λ=874nm), Periodic (λ=855nm).

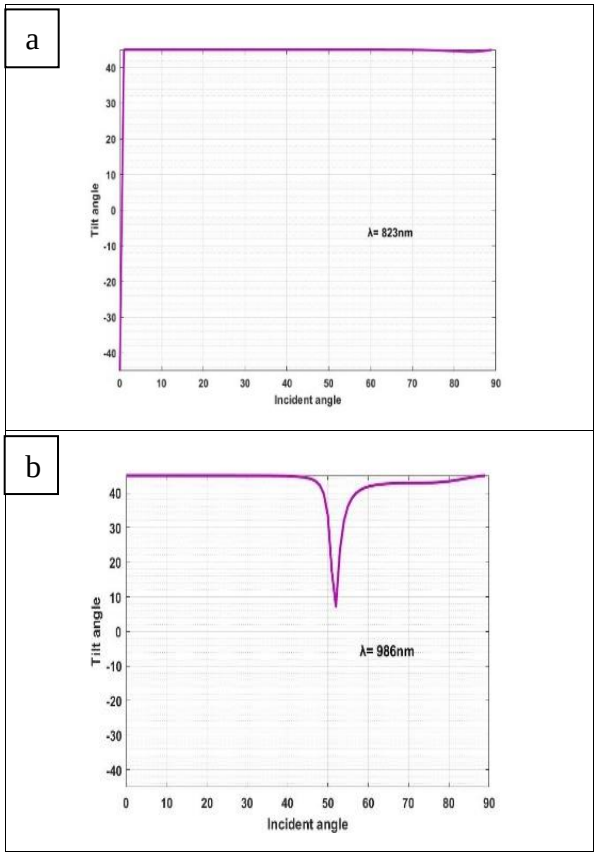

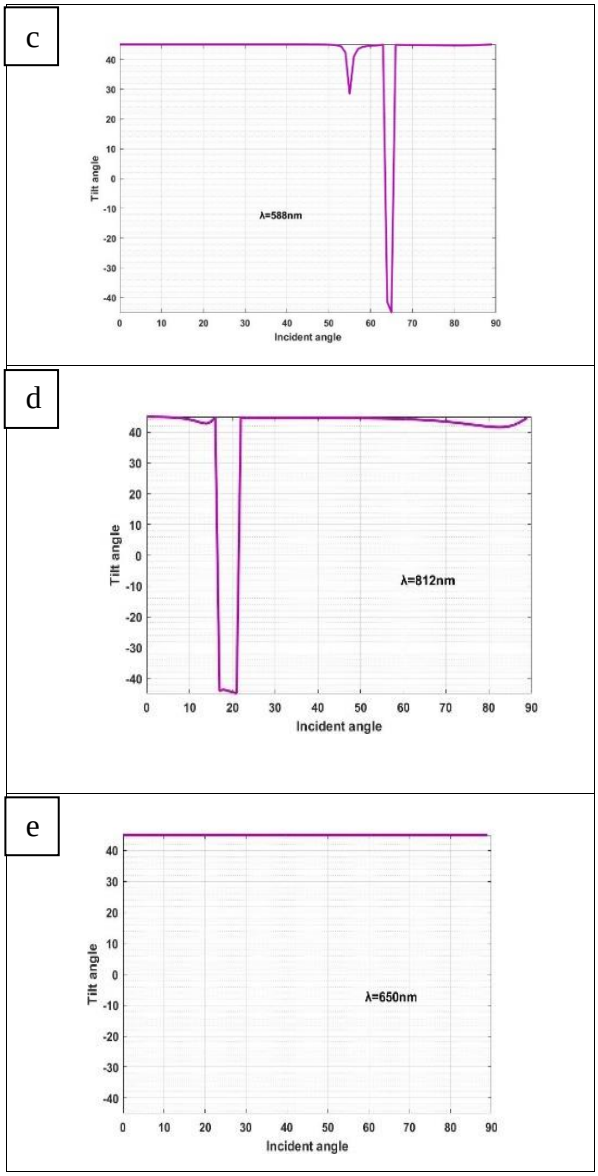

Figure 7. *The center edge's tilt angle of reflection in relation to the entering light's wavelength* Fibonacci (λ=823nm), Thue-Morse (λ=986nm), Double Period (λ = 588 nm), Rudin Shapiro (λ=812nm), Periodic (λ=650nm).

Figure 8 makes it abundantly evident that the band gap is a region through which electromagnetic waves are unable to travel, but instead, they are reflected. Within the context of this plot, we have selected a wavelength that is located in the middle of the band gap and has the greatest degree of reflection. In the figure, it is evident that the tilt angle has not changed with the rise in the incidence angle for the Fibonacci sequence and the periodic structure. On the other hand, as the angle of incidence grows to a certain degree, the slope angle of structures like the T Morse, Double Period, and Rudin Shapiro begins to

alter in some regions. Meta surfaces are much sought after for their potential use in polarization control and tuning. In many optical applications, including ellipsometry, polarimetry, optical sensing, and polarization-division multiplexing, polarization manipulation is essential. This manipulation enhances performance compared to traditional methods of material characterization and communication.

LIMITATIONS

Limitations occur in all types of research, and most are beyond the researcher's control (due to practical constraints such as budget and lack of research tools or access to the population of interest).

CONCLUSION

This study demonstrates the potential of one-dimensional photonic crystals with fullerene and tellurium nanolayers in achieving precise phase and polarization control of electromagnetic waves. By leveraging periodic and quasiperiodic structures, such as Fibonacci and Thue-Morse, the research highlights their efficacy in generating tunable photonic bandgaps across the visible to near-infrared spectrum. The findings emphasize the suitability of these structures as polarization filters and phase modulators, with applications in optical devices and sensors. The use of the transfer matrix method further underscores the robustness of the design in manipulating light polarization and achieving desired electromagnetic properties with high precision. These insights open pathways for advanced applications and continued exploration of photonic crystal technologies.

AUTHORS CONTRIBUTION

SSK: Conception and Design. **SLA, SAA,** and **SOA**: Data Collection. **SSK**: Analysis and Interpretation of Data. **SSK**: Critical Revision of the Article for Important Intellectual Content. **All authors**: Final Approval of the Version to Be Published.

ACKNOWLEDGEMENTS

We thank [Department of Physics] for their assistance with data collection and analysis.

REFERENCES

[1] E. Yablonovitch, "Inhibited spontaneous emission in solid-state physics and electronics," *Phys Rev Lett* 58, 1987, doi: https://doi.org/10.1103/PhysRevLett.58.2059.

[2] S. John, "Strong localization of photons in certain disordered dielectric superlattices," *Phys Rev Lett* 58, 1987, doi: https://doi.org/10.1103/PhysRevLett.58.2486.

[3] P. Yeh, M. Hendry, "Optical Waves in Layered Media," *Phys Today* 43, 1990, doi: https://doi.org/10.1063/1.2810419.

[4] Y. Trabelsi, N. B. Ali, F. Segovia-Chaves, et al, "Photonic band gap properties of one-dimensional photonic quasicrystals containing Nematic liquid crystals," 2020, *Results Phys* 19, doi: https://doi.org/10.1016/j.rinp.2020.103600.

[5] M. Bellingeri, F. Scotognella, A. Chiasera, et al, "One-dimensional disordered photonic structures with two or more materials," 2018, doi: 10.48550/arXiv.1803.11375.

[6] S. Wang, X. Yang, C. T. Liu, "Omnidirectional reflection in one-dimensional ternary photonic crystals and photonic heterostructures," *Physics Letters, Section A: General, Atomic and Solid State Physics* 378, 2014, doi: 10.1016/j.physleta.2014.03.010.

[7] A. N. Poddubny, E. L. Ivchenko "Photonic quasicrystalline and aperiodic structures," *Physica E Low Dimens Syst Nanostruct* 42, 2010, doi: https://doi.org/10.1016/j.physe.2010.02.020.

[8] F. Segovia-Chaves F, Y. Trabelsi, T.A. Taha, "Coupling photonic quasicrystals with a one-dimensional critical high-temperature superconducting cavity," *Optik*

(Stuttg) 281, 2023, doi: 10.1016/j.ijleo.2023.170847.

[9] M. Song, W. Jin W, S. Fu, et al, "Light wave propagation and diffraction inhibition in three-dimensional photonic quasicrystal lattices," *Results Phys* 52, doi: https://doi.org/10.1016/j.rinp.2023.106884.

[10] Y. Bouazzi, K. Kanzari, "Interferential polychromatic filters based on the quasi-periodic one-dimensional generalized multilayer Thue-Morse structures," *Optica Applicata* 39, 2009.

[11] Y. Trabelsi, F. Segovia-Chaves, N. B. Ali, "Tunable defect modes through the (YBCO-Yttria) based on Octonacci photonic quasicrystals," *Results Phys* 44, 2023, doi: https://doi.org/10.1016/j.rinp.2022.106176.

[12] S. Zirak-Gharamaleki S, "Narrowband optical filter design for DWDM communication applications based on Generalized Aperiodic Thue-Morse structures,"*Opt Commun* 284, 2011, doi: https://doi.org/10.1016/j.optcom.2010.09.045.

[13] H. Rahimi, "Analysis of photonic spectra in Thue-Morse, double-period and Rudin-Shapiro quasiregular structures made of high temperature superconductors in visible range," *Opt Mater (Amst)* 57, 2016, doi: 10.1016/j.optmat.2016.04.022.

[14] J Wu, "TPP-assisted multi-band absorption enhancement in graphene based on Fibonacci quasiperiodic photonic crystal," *Results Phys* 33, 2022, doi: https://doi.org/10.1016/j.rinp.2022.105210.

[15] H. F. Zhang, J. P. Zhen, W. P. He, "Omnidirectional photonic band gaps enhanced by Fibonacci quasiperiodic one-dimensional ternary plasma photonic crystals," *Optik (Stuttg)* 124, 2013, doi: 10.1063/1.4765063.

[16] C. H. Costa, M. S. Vasconcelos, U. L. Fulco, et al, "Thermal radiation in one-dimensional photonic quasicrystals with graphene," *Opt Mater (Amst)* 72, 2017, doi: https://doi.org/10.1016/j.optmat.2017.07.029.

[17] B. K. Singh, P. C. Pandey, "Influence of graded index materials on the photonic localization in one-dimensional quasiperiodic (Thue-Mosre and Double-Periodic) photonic crystals," *Opt Commun* 333, 2014, doi: https://doi.org/10.1016/j.optcom.2014.07.043.

[18] H. A. Gómez-Urrea, J. Escorcia-García, C. A. Duque, et al, "Analysis of light propagation in quasiregular and hybrid Rudin–Shapiro one-dimensional photonic crystals with superconducting layers," *Photonics Nanostruct* 27, 2017, doi: https://doi.org/10.1016/j.photonics.2017.08.001.

[19] F. Segovia-Chaves, H. A. Elsayed, "Transmittance spectrum in a Rudin Shapiro quasiperiodic one-dimensional photonic crystal with superconducting layers," *Physica C: Superconductivity and its Applications* 587, 2021, doi: 10.1016/j.physc.2021.1353898.

[20] N. T. K. Thanh, S. J. A. Biggs, Darr, "Philosophical Transactions of the Royal Society A: Mathematical, Physical and Engineering Sciences: Preface," *Philosophical Transactions of the Royal Society A: Mathematical, Physical and Engineering Sciences* 368, 2010, doi: https://doi.org/10.1098/rsta.

[21] S. K. Tiwari, V. Kumar, A. Huczko, et al, "Magical Allotropes of Carbon: Prospects and Applications," *Critical Reviews in Solid State and Materials Sciences* 41, 2016, doi: https://doi.org/10.1080/10408436.2015.1127206.

[22] P. S. Karthik, A. L. Himaja, S. P. Singh, "Carbon-allotropes: Synthesis methods, applications and future perspectives," *Carbon Letters* 15, 2014, doi: 10.5714/CL.2014.15.4.219.

[23] K. Tanigaki, I. Hirosawa, T. W. Ebbesen, et al, "Superconductivity in sodium-and lithium-containing alkali-metal

fullerides," *Nature* 356, 1992, doi: https://doi.org/10.1038/356419a0.
[24] M. J. Rosseinsky, A. P. Ramirez, S. H. Glarum, et al, "Superconductivity at 28 K in Rb C60," *Phys Rev Lett* 66, 1999, doi: https://doi.org/10.1103/PhysRevLett.66.2830.
[25] W. Krätschmer, L. D. Lamb, "Fostiropoulos K, et al, Solid C60: a new form of carbon," *Nature* 347, 1990, doi: https://doi.org/10.1038/347354a0.
[26.] Q. Xue, Y. Ling, T. Ogino, et al, "C60 single crystal films on GaAs(001) surfaces," *Thin Solid Films* 281–282, 1996, doi: https://doi.org/10.1016/0040-6090(96)08710-X.
[27] F. Akkurt, "Laser induced electro-optical characterization of anthraquinone dye and fullerene C60 doped guest-host liquid crystal systems," *J Mol Liq* 194, 2014, doi: https://doi.org/10.1016/j.molliq.2014.02.040.
[28] E. V. Maistruk, I. P. Koziarskyi, D. P. Koziarskyi, et al, "Electrical properties of the Cu 2 O/Cd 1 - x Zn x Te heterostructure," *Journal of Nano- and Electronic Physics* 11, 2019, doi: https://doi.org/10.21272/jnep.11(2).02007.
[29] S. K. Srivastava, S. P. Ojha, "Omnidirectional reflection bands in one-dimensional photonic crystal structure using fullerene films," *Progress in Electromagnetics Research* 74, 2007, doi: https://doi.org/10.2528/PIER07050202.
[30] E. Giudice, E. Magnano, S. Rusponi, "Morphology of C60 thin films grown on Ag(001)," *Surf Sci* 405, 1998, doi: https://doi.org/10.1016/S0039-6028(98)00171-X.
[31] P. Han, B. Xu, J. Liang, et al, "Band gaps of two-dimensional photonic crystal structure using fullerene films," *Physica E Low Dimens Syst Nanostruct* 25, 2004, doi: https://doi.org/10.1016/j.physe.2004.05.009.
[32] C. J. Wu, "Transmission and reflection in a periodic superconductor/dielectric film multilayer structure," *J Electromagn Waves Appl* 19, 2005, doi: https://doi.org/10.1163/156939305775570468.
[33] X. Bingshe, H. Peide, W. Liping, et al, "Optical properties in 2D photonic crystal structure using fullerene and azafullerene thin films," *Opt Commun* 250, 2005, doi: https://doi.org/10.1016/j.optcom.2005.02.017.
[34] H. Rahimi, "The Highest and Lowest Photonic Bandwidths, Absorption Coefficients and Field Localizations among Common 1D Quasiperiodic Structures Containing Graphene and Silicon Dioxide," *Silicon* 12, 2020, doi: https://doi.org/10.1007/s12633-019-00132-6.
[35] Z. Saleki, S. R. Entezar, A. Madani, "Optical properties of a one-dimensional photonic crystal containing a graphene-based hyperbolic metamaterial defect layer," *Appl Opt* 56, 2017, doi: https://doi.org/10.1364/AO.56.000317.
[36] H. Rahimi, A. Namdar, S. Roshan Entezar, et al, "Photonic transmission spectra in one-dimensional fibonacci multilayer structures containing single-negative metamaterials," *Progress in Electromagnetics Research* 102, 2010, doi: https://doi.org/10.2528/PIER09122303.
[37] M. Mantela, K. Lambropoulos, M. Theodorakou, et al, Quasi-periodic and fractal polymers: Energy structure and carrier transfer," *Materials* 12, 2019, doi: https://doi.org/10.3390/ma12132177.
[38] I. M. Felix, L. F. C. Pereira, "Thermal conductivity of Thue–Morse and double-period quasiperiodic graphene-hBN superlattices," *Int J Heat Mass Transf* 186, 2022, doi: https://doi.org/10.1016/j.ijheatmasstransfer.2021.122464.
[39] A. Biswal, "Periodic and quasi-periodic one-dimensional extrinsically magnetized photonic crystals with robust photonic bandgaps," *Appl Opt* 62, 2023, doi: https://doi.org/10.1364/AO.502541.
[40] A. Dell, A. Krynkin, K. V. Horoshenkov, "The use of the transfer matrix method to predict the effective fluid properties of acoustical systems," *Applied Acoustics*

182, 2021, doi: https://doi.org/10.1016/j.apacoust.2021.108259.

[41] T. Zhan, X. Shi, Y. Dai, et al, "Transfer matrix method for optics in graphene layers," *Journal of Physics Condensed Matter* 25, 2013, doi: https://doi.org/10.1088/0953-8984/25/21/215301.

[42] B. D. Smith, S. H. Ward, "on the computation of polarization ellipse parameters," *Geophysics* 39, 1974, doi: https://doi.org/10.1190/1.1440474.

[43] A. Biswal, R. Kumar, C. Nayak, et al, "Photonic bandgap characteristics of GaAs/AlAs-based one-dimensional quasi-periodic photonic crystal," *Optik (Stuttg)* 234, 2021, doi: https://doi.org/10.1016/j.ijleo.2021.166597.

[44] O. Habli, J. Zaghdoudi, M. Kanzari, "Omnidirectional photonic band gap based on nonlinear periodic and quasi-periodic photonic crystals," *Appl Phys B* 128, 2022, doi: https://doi.org/10.1007/s00340-022-07845-4.

[45] X. Li, Q. Kong, X. Wang, et al, "Transmission properties in Fibonacci quasi-periodic photonic crystal containing negative-zero-positive index metamaterials," *Commun Theor Phys* 75, 2023, doi: https://doi.org/10.1088/1572-9494/acb3b6.

[46] C. Dong, Y. Zheng, K. S. Shen, et al, "Polarization-independent wide-angle flexible multiband thermal emitters enabled by layered quasi-periodic photonic crystal". *Opt Laser Technol* 156, 2022, doi: https://doi.org/10.1016/j.optlastec.2022.108474.